Biophysical Chemistry, 35 (1990) 165–178
Elsevier

BIOCHE 01421

How does cisplatin alter DNA structure?

A molecular mechanics study on double-stranded oligonucleotides

Jiří Kozelka and Jean-Claude Chottard

Laboratoire de Chimie et Biochimie Pharmacologiques et Toxicologiques, Unité associée au CNRS no. 400, Université René Descartes, 45 rue des Saints-Pères, 75270 Paris Cedex 06, France

Received 25 May 1989
Accepted 6 September 1989

Antitumor drug; Cisplatin; DNA structure; Molecular mechanics

Molecular models for two double-stranded decanucleotides, d(GCCG*G*ATCGC)-d(GCGATCCGGC) (**1**) and d(GCTG*G*ATCGC)-d(GCGATCCAGC) (**2**), with the G* guanines cross-linked by a *cis*-$Pt(NH_3)_2$ moiety, were calculated using molecular mechanics. Nine models for **1** and eight models for **2** are reported; in all of them, the double helix is kinked by approx. 60° towards the major groove and slightly unwound. The model building has been guided by comparison with the NMR data available for duplex **1**. The influence of the base at the 5′-side of the coordinated G*G* dinucleotide is discussed.

1. Introduction

The major adduct formed between the antitumor drug *cis*-$[PtCl_2(NH_3)_2]$ (cisplatin) and DNA is the intrastrand GpG chelate [1]. The GpG preference also holds for single-stranded [2] and double-stranded [3] oligonucleotides, which are used as model compounds for DNA. The formation of XpG platinum chelates (X = A, G) correlates with antitumor activity [4]. It is possible (although not proven) that the GpG cross-link is the origin of the antitumor properties of cisplatin. Such a hypothesis is quite plausible, since the *trans* isomer of cisplatin, which cannot cross-link adjacent nucleobases for geometric reasons, does not exhibit any antitumor activity [5]. A discussion of the biological role of the GpG chelate requires detailed knowledge of the deformation of DNA caused by the platinum complex.

Two recent crystal structure determinations of *cis*-$Pt(NH_3)_2$ adducts of short, single-stranded oligonucleotides have yielded valuable insights into the way in which platinum binds to a GpG fragment [6,7]. However, the geometric constraints of a double helix are quite different from those of a single strand, making structural predictions for duplexes from the X-ray data problematic.

Molecular mechanics has become a useful tool for conformational analyses. This method, based on the minimization of the conformational energy, yields structures that are energetically feasible. Usually, a number of energy-minimized structures emerge, and hence, experimentally determined physical data are necessary for the selection of the correct model(s).

The first molecular mechanics calculations performed on double-stranded, GpG-platinated oligonucleotides yielded three model structures: one, in which the double helix was only locally

Correspondence address: J. Kozelka, Laboratoire de Chimie et Biochimie Pharmacologiques et Toxicologiques, Unité associée au CNRS no. 400, Université René Descartes, 45 rue des Saints-Pères, 75270 Paris Cedex 06, France.

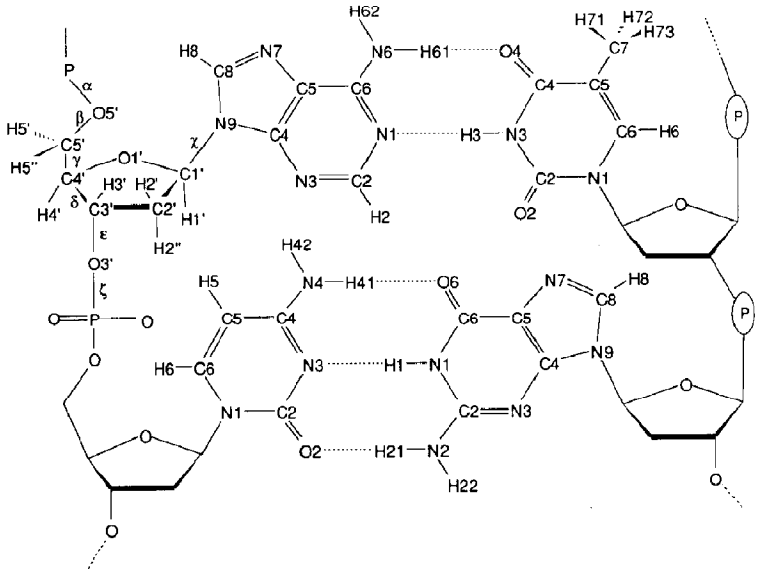

Fig. 1. Numbering of atoms and labeling of torsional angles.

perturbed, and two others, where the helix axis was kinked [8]. The models had comparable energies and all were in accord with NMR data available at that time. We shall report elsewhere a detailed NMR and molecular mechanics study on the decanucleotide duplex d(GCCG*G*ATCG-C)-d(GCGATCCGGC) (**1**), platinated on the N7 atoms of the G* guanines. Simultaneous consideration of chemical shifts, coupling constants and intensities of the nuclear Overhauser effects (NOEs) allowed us to rule out the possibility of the unkinked model and to discover a novel family of kinked structures, which, as we have shown, could be involved in an equilibrium with the family of kinked models reported earlier as 'Model C' [9]. Each of these families corresponded to an ensemble of interconverting structures. Since we did not have enough computer power for a sufficiently long molecular dynamics simulation, we have considered nine distinct models, for which the relevant chemical shifts, coupling constants, and interatomic distances were calculated. The experimental data were in agreement with an equilibrium between these nine structures [9].

The present article first explores the nine models for duplex **1** focusing on structural information that is not directly related to NMR observable parameters such as the geometry of the kink, interplanar angles between bases, and hydrogen bonding with the ammine ligands of platinum. The second part of the paper concerns the question of the manner in which variations of the bases adjacent to the coordinated G*G* fragment modify the structure of the models and

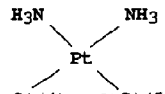

G(1)p(2)C(2)p(3)C(3)p(4)G*(4)p(5)G*(5)p(6)A(6)p(7)T(7)p(8)C(8)p(9)G(9)p(10)C(10)

C(20)p(20)G(19)p(19)G(18)p(18)C(17)p(17)C(16)p(16)T(15)p(15)A(14)p(14)G(13)p(13)C(12)p(12)G(11)

Scheme 1.

influence their relative energies. We present here molecular models for a derivative of duplex **1** in which the cytosine C(3) (the base 5′ to the coordinated G*G* dinucleotide) was replaced by a thymine (duplex **2**).

The unkinked model ('Model A') reported previously [8a,8c] is not considered in the current article, since the experimental data are not in support of such a structure [9].

The residue numbering is shown in scheme 1. The numbering of atoms within the nucleotides (fig. 1) is according to the nomenclature of the IUPAC recommendations [10] throughout the paper, except for the hydrogen atoms on carbons C2′ and C5′, for which the notation H2′, H2″, H5′ and H5″ was used rather than the unfamiliar symbols H2′1, H2′2, etc.

2. Experimental

Energy minimization of the structures was performed using the program AMBER [11]. Details of the force field have been described previously [9]. The charges used for the *cis*-$Pt(NH_3)_2$ residue were those of the force-field 'HIGH' [9]. Counterions and solvent molecules were not included in calculations.

The kink angle and the helical unwinding were calculated according to the system depicted in fig. 2. The orientations of the two halves of the kinked helix were defined using two blocks of atoms: the lower block comprised bases 6–15, the upper block containing bases 1–2 and 19–20. Those at the kink site, i.e., bases 3–5 and 16–18, were not used, since they are excessively perturbed in the platinated models. The refined unplatinated duplex served as reference. The lower block of the investigated structure was least-squares fitted into the reference structure, so that its helix axis coincided with the axis z of the reference helix. Subsequently, a computer program searched for the rotational angles θ and ψ orienting the upper block of the reference structure such that it gave the best least-squares fit with the upper block of the kinked structure. The first rotation by θ (kinking) transformed the helix axis z of the reference structure into the axis of the upper part of the kinked helix, z'. The rotational axis for this case, k, lay in the xy plane and its angle with the y axis, ϕ, was employed as a third variable. The second rotation by ψ (unwinding) turned the kinked upper block about its own axis z'.

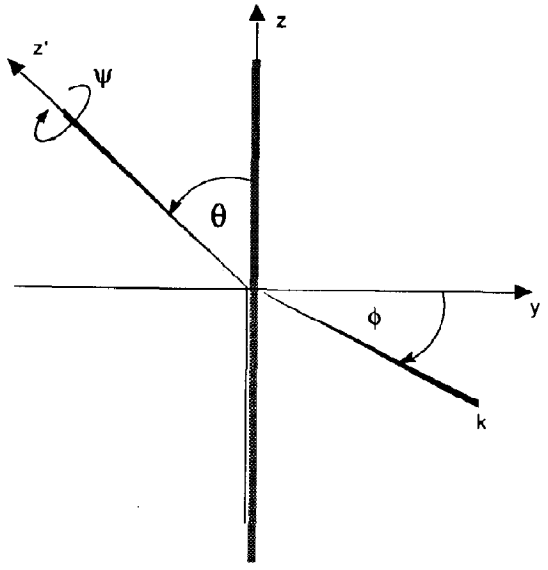

Fig. 2. The system of axes defining the kink angle θ, the helical unwinding ψ, and the kink direction ϕ. z: helix axis of the reference helix (cross-hatched bar) coinciding with the axis of the lower part of the kinked helix. The axis of the upper part, z', results from a rotation of z about k which is perpendicular to z. The angle ϕ gives the position of k in the xy plane. The y axis has been chosen to be parallel to the projection of the C(16)C6-G*(5)C8 vector into the xy plane [13] (fig. 3). Since the G*(5)-C(16) base-pair is situated just at the kink site, $\phi = 0°$ corresponds to kinking straight into the major groove ($\theta < 0°$) or into the minor groove ($\theta > 0°$). Positive ϕ values signify that the y axis has been rotated about the z axis in a counterclockwise direction to give the k axis; positive ψ values correspond to unwinding of a right-handed helix. In the case depicted, ϕ is negative and θ positive.

3. Results and discussion

3.1. Structural aspects of the molecular models for the platinated duplex 1

3.1.1. General features

In all models, the double helix is kinked by 55–62° towards the major groove and unwound

by 12–19°. The primary cause of the kink is the interplanar angle subtended by the two coordinated guanines (48–55°). This interplanar angle is considerably smaller than that found in the crystals of single-stranded GpG adducts of *cis*-$Pt(NH_3)_2$ (76–87°) [6b,7]. This difference reflects the fact that the constraints of the double helix are much stronger than those of a single helix. For platinum coordination, the ideal guanine-guanine angle would be 90°.

There is little distortion of the square planar geometry around the platinum atom. The N7-Pt-N7 angle is always less than 90° (ranging between 84.8 and 86.1°), whereas the other three *cis*-N-Pt-N angles are within the range 90.4–93.0°. The *trans*-N-Pt-N angles range between 166.1 and 176.7°. The atoms of the platinum coordination plane deviate by less than 0.18 Å from the least-squares plane.

A general feature of all G*pG* platinated models is an N pucker [10,13] of the 5′-G* guanosine. The pucker is a direct consequence of the platinum coordination. The two cross-linked N7 atoms are forced to lie at a distance of approx. 2.8 Å, which is considerably shorter than their separation in the unperturbed B-DNA helix (4.1 Å). The S → N repuckering on the 5′ guanosine reduces the O3′–O5′ distance on this nucleotide and thus helps to accommodate the backbone contraction. The N sugar pucker on the 5′-G* has been observed in all single- and double-stranded GpG platinated oligonucleotides structurally characterized, in solution [14] as well as in crystals [6,7].

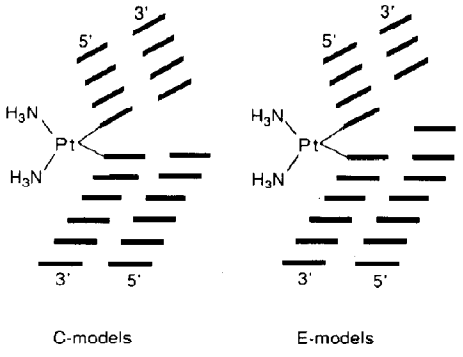

Scheme 2.

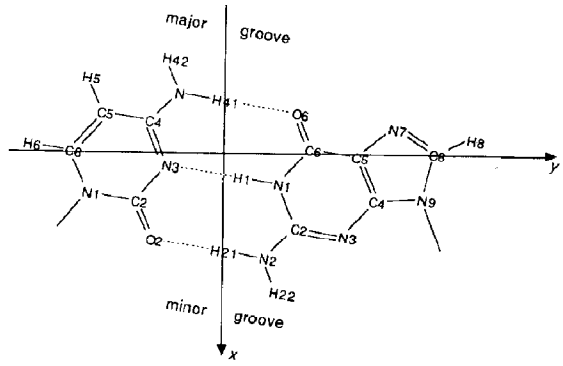

Fig. 3. The coordinate system of a GC base-pair.

The unplatinated strand can accommodate the kink in the platinated strand in either of two ways: in one family of models, designated as C-models, the unplatinated strand is kinked at the same site, i.e., between the two cytosines complementary to the platinated G*pG* dinucleotide. In the other, referred to as E-models, the kink in the unplatinated strand is shifted one nucleotide towards the 3′ end (scheme 2) [9].

Two selected models, one each of the C- and E-families, are depicted in fig. 4.

*3.1.2. Ammine-phosphate hydrogen bonds and the sugar pucker of the nucleotide 5′ to G*pG**

The kinking of the helix brings the two phosphate groups at the 5′ side of the platinated G*pG* moiety, i.e., p(4) and p(3), in proximity to one ammine ligand of the platinum, so that this ammine ligand can be hydrogen-bonded to either p(4) or both p(4) and p(3). This is possible in both model families C and E. In order to distinguish between the different model variants, we use a numerical index indicating the number of ammine-phosphate hydrogen bonds. For instance, C_1 represents the C-model having one ammine-phosphate hydrogen bond to p(4).

The hydrogen bonding between NH_3 and phosphate p(4) creates a repulsive contact between this NH_3 ligand and the C(3)C2′ methylene (shortest H ··· H distance, 2.11 Å) (fig. 5b). The sugar of this nucleotide avoids such repulsion by repuckering from S to N; this repuckering results in bulging, thus moving the C2′ atom away from the

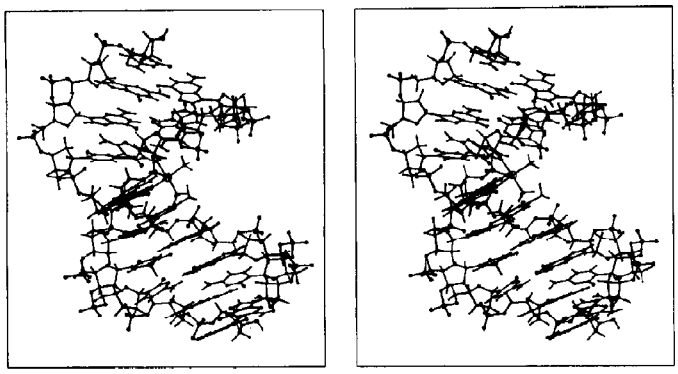

(a) Model $C_{\cdot}$

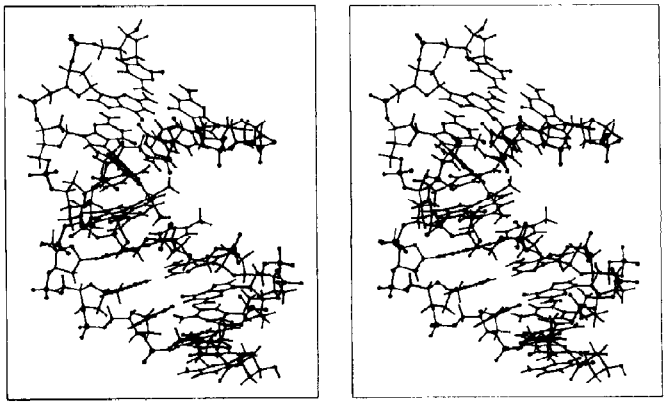

(b) Model E_{1A}

Fig. 4. Stereoview of two selected models for duplex **1**.

ammine ligand, as seen in fig. 5a. This short contact is absent in the models lacking ammine-phosphate hydrogen bonds, i.e., C_0 and E_0. Here, the sugar pucker on nucleotide C(3) can be N or S. Thus, we can distinguish among the models C_{0N} and C_{0S}, and E_{0N} and E_{0S}, where the subscript N or S refers to the corresponding type of sugar pucker on nucleotide C(3).

It should be noted that in aqueous solution, the ammine and phosphate residues are able to interact not only by direct hydrogen bonding but also through a water molecule. Recent quantum-chemical calculations on the interaction of a dihydrogenophosphate anion with ammonia yielded similar values for the energy of direct and water-mediated hydrogen bonding [15]. Since our calculations do not involve solvent molecules, the conformational energies that are evaluated cannot be used to predict the relative stabilities of the model structures in solution. However, from comparison of the angles of pseudorotation [10,13] for cytidine C(3) with the observed $J_{1'2'}$ and $J_{1'2''}$ coupling constants, it can be concluded that structures of duplex **1** with zero, one and two ammine-phosphate hydrogen bonds exist side by side [9].

3.1.3. Kink angle and unwinding of the helix

The kink angle (θ), unwinding angle (ψ) and direction of the kink (ϕ) are listed in table 1 for all the models (angles defined in section 2 and fig. 2). One observes that platinum coordination kinks the double helix by 55–62° towards the major groove, and unwinds it by 12–19°. The variations in θ, ψ and ϕ between the different models are

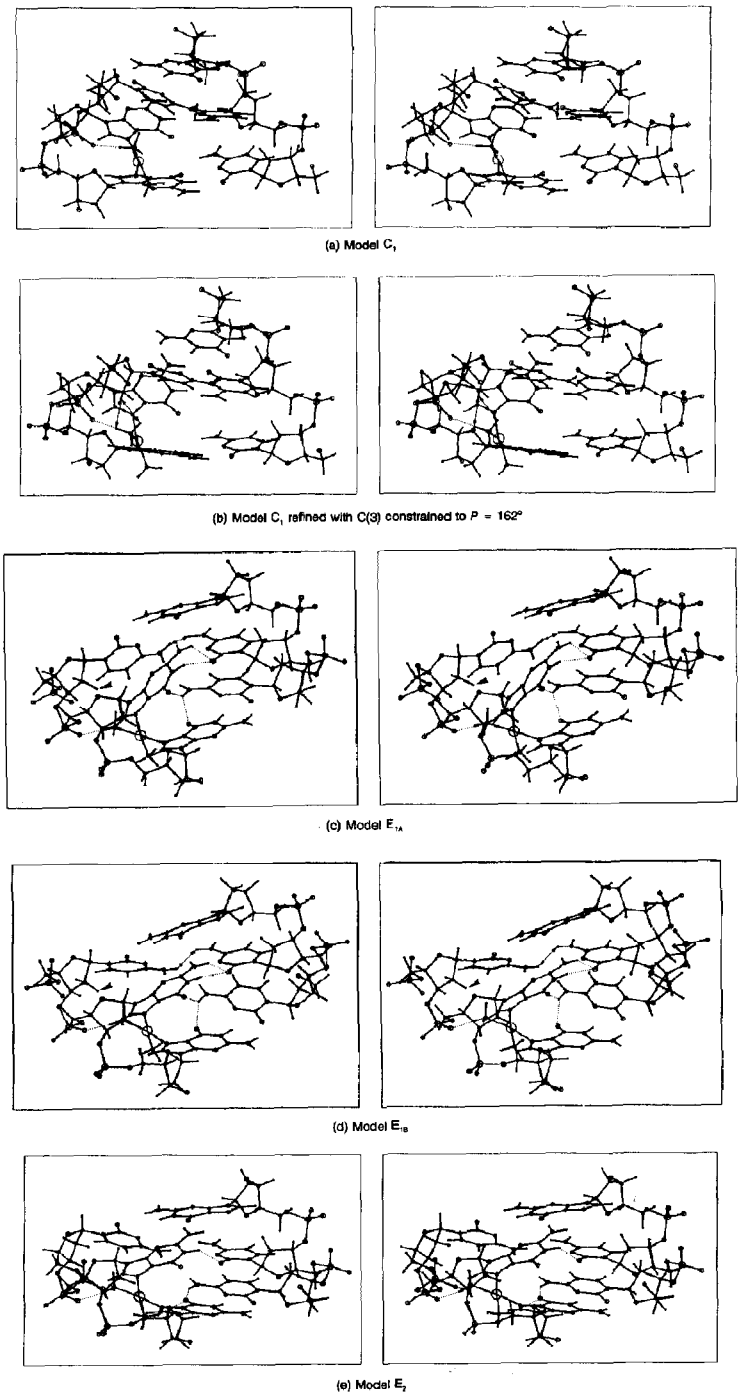

Fig. 5. Stereoview of the central part of duplex **1**, comprising the nucleotides 3–5 and 16–18. Dashed lines indicate hydrogen bonds discussed in the text; double arrows denote short contacts; the simple arrow (c,d) identifies the H2′ proton of cytidine C(3).

small in extent except for model E_1. In this case, two variants designated E_{1A} and E_{1B}, have been found. Whereas model E_{1B} has θ, ψ and ϕ parameters of similar values to those of the other models, model E_{1A} is clearly distinct in having a ϕ value of 26° and an unwinding angle which is somewhat smaller than that of the others. The different kink direction ϕ in model E_{1A} has several structural consequences. One of these is the position of the C(3) sugar with respect to the guanine G*(4). Comparison with model E_{1B} (fig. 5c and d) shows that in model E_{1A}, the sugar of C(3) is located closer to the guanine G*(4), with its H2′ atom penetrating through the shielding cone of G*(4). Experimentally, significant shielding has indeed been demonstrated for this proton, and in fact this observation led us to the development of model E_{1A} [9].

3.1.4. Base-pairing

The C-models are characterized by intact Watson-Crick base-pairing, including the coordinated G*pG* moiety (fig. 5a). In the E-models, on the other hand, cytosine C(17) subtends a considerable interplanar angle with its counterpart, guanine G*(4), so that their Watson-Crick base-pairing is disrupted. Compensation for the disrupted Watson-Crick base-pairing comes from two bifurcated hydrogen bonds: one connecting the O2 atom of C(17) with the H21 and H1 protons of G*(4), and the other, bifurcating from the H41 proton of C(16) to the O6 atoms of G*(4) and G*(5) (fig. 5c and d). In contrast, model E_2 does not form such bifurcated hydrogen bonds. Instead, G*(5) is perfectly coplanar and Watson-Crick hydrogen-bonded to C(16), and C(17) forms only a weak hydrogen bond from its O2 atom to G*(4)H1 (fig. 5e).

3.1.5. Sugar puckers

Apart from the N puckers observed on the platinated strand (vide supra), kinking of the helix is reflected in S → N repuckering on one or two nucleotides of the unplatinated strand. Inspection of the angles of pseudorotation given for the principal residues in table 1 (row denoted sugar puckers) shows that the C(16) : C(17) dinucleotide, i.e., the dinucleotide complementary to G*pG*, assumes the N : S pucker type in the C-models, whereas in the E-models, the pucker type is S : N or N : N. Thus, either one or two nucleotides at the 5′ side of a kink assume the N pucker. A similar result has emerged from modeling of kink sites on double-stranded B-DNA reported by Sobell et al. [17,18].

3.1.6. Sugar-phosphate backbone

Inspection of the torsional angles along the sugar-phosphate backbone (table s1, see. p. 177) reveals that drastic changes in these angles do not occur on platinum coordination. This demonstrates the flexibility of the DNA backbone, which is capable of accommodating even quite large helix deformations while retaining its usual torsional angles.

Nevertheless, we have obtained evidence indicating that platinum coordination exerts a significant influence on the thermodynamics of the backbone at the nucleotide G*(5), concerning the torsional angles α and γ (fig. 1). These torsional angles usually assume the $\alpha(gauche^-) - \gamma(gauche^+)$ [10,13] ($\alpha^-\gamma^+$) conformation in a B-DNA helix, the alternative $\alpha(trans) - \gamma(trans)$ [10,13] ($\alpha^t\gamma^t$) conformation being somewhat less stable. In the energy-minimized unplatinated duplex **1**, for instance, the G*(5) $\alpha^t\gamma^t$ conformation is 2.6 kcal/mol less stable than the standard G*(5) $\alpha^-\gamma^+$ conformation. Calculation of the energies for both G*(5) $\alpha^-\gamma^+$ and $\alpha^t\gamma^t$ variants of all platinated models of **1** revealed that the difference in energy is significantly diminished (table 1, middle part), and for model E_{1A}, the order is even reversed.

The finding that GpG platination can displace the $\alpha^-\gamma^+ \rightleftarrows \alpha^t\gamma^t$ equilibrium for the 3′-guanosine to the right ($\alpha^t\gamma^t$) is quite important, since the α^t conformation could account for the downfield shift observed for the ^{31}P-NMR resonance of the G*pG* phosphate in all known GpG-platinated oligonucleotides [19,20]. In fact, of the seven crystallographically characterized molecules containing the platinum-cross-linked d(GpG) moiety, one shows an $\alpha^t\gamma^t$ conformation on the 3′-guanosine (molecule 3 of *cis*-[Pt(NH_3)$_2${d(CpGpG)}] [7], and for one, disorder between $\alpha^-\gamma^+$ and $\alpha^t\gamma^t$ has been found (molecule 2 of *cis*-[Pt(NH_3)$_2${d(pG-

pG)}] [6b]. Such disorder strongly suggests that the conformational energies are comparable and that in solution equilibrium is attained.

An $\alpha^t\gamma^t$ conformation has recently been observed at two sites of the crystallized doubly kinked RNA duplex $[U(UA)_6A]_2$; interestingly, both $\alpha^t\gamma^t$

Table 1

Geometric parameters and energies of the models for duplex 1 [a]

	Model								
	C_{0N}	C_{0S}	C_1	C_2	E_{0N}	E_{0S}	E_{1A}	E_{1B}	E_2
Final energy	−189.1	−185.3	−190.4	−188.5	−190.4	−187.6	−190.2	−191.8	−189.0
Kink angle (θ) [d]	−62	−55	−58	−60	−56	−56	−56	−60	−61
Unwinding (ψ) [d]	16	16	17	17	17	15	12	16	19
Kink direction (ϕ) [d]	6	3	4	−5	4	6	26	7	−1
Interplanar angles									
C(2)/C(3)	3.8	4.2	5.1	31.7	6.0	1.8	12.8	7.9	29.9
C(3)/G*(4)	19.2	20.7	22.7	28.3	26.7	21.4	23.0	29.4	28.9
G*(4)/G*(5)	52.7	48.3	52.5	50.3	47.9	49.1	54.9	53.4	49.0
G*(5)/A(6)	11.8	11.8	11.0	12.6	10.0	11.6	11.8	11.6	8.8
C(3)/G(18)	18.5	11.4	17.9	26.1	21.1	14.9	25.2	21.2	18.9
G*(4)/C(17)	29.8	29.5	28.8	27.3	50.5	50.5	64.0	51.8	53.0
G*(5)/C(16)	20.4	17.9	16.7	22.5	17.2	17.6	14.1	20.3	9.9
C(16)/C(17)	40.6	35.8	38.8	40.1	16.9	18.2	4.6	21.8	4.5
C(17)/G(18)	12.1	8.0	10.6	7.6	36.7	36.8	35.8	35.2	33.2
G*(4)/PtN_4 [b]	71.8	76.1	66.2	55.5	71.9	73.5	78.1	65.6	54.8
G*(5)/PtN_4 [b]	68.9	71.3	65.2	56.7	73.2	70.8	74.5	63.9	59.3
Conformation of G*(5) $\alpha\ \gamma$	g−g+	g−g+	g−g+	g−g+	g−g+	g−g+	tt	g−g+	g−g+
Energy difference for $\alpha^-\gamma^+ \rightarrow \alpha^t\gamma^t$	+1.1	+1.7	+1.2	+1.6	+1.2	+0.7	−0.1	+1.3	+1.0
Sugar puckers [c]									
C(2)	127	128	127	140	128	125	71	126	138
C(3)	31	132	28	−9	27	103	30	22	−10
G*(4)	22	35	12	12	21	37	4	12	12
G*(5)	137	138	129	131	138	136	150	132	134
C(16)	31	30	32	32	34	33	150	31	143
C(17)	148	149	146	149	25	23	37	23	32
Distance of Pt from G*(4)	0.57	0.69	0.51	0.51	0.72	0.78	0.47	0.51	0.48
Distance of Pt from G*(5)	0.39	0.42	0.44	0.39	0.43	0.31	0.47	0.41	0.38
Shortest NH···O separations									
NH···p(3)	5.08	6.13	5.31	1.97	5.63	6.77	4.44	5.14	1.88
NH···p(4)	3.55	5.17	1.90	2.03	3.25	5.28	1.82	1.92	1.92
NH···G*(5)O6	2.53	2.60	2.62	2.17	2.68	2.63	2.91	2.71	2.10
NH···T(15)O4	2.03	1.93	2.33	3.30	1.96	1.97	1.89	2.07	3.61
Non-bonding distance C(3)H41···C(17)H41	2.05	2.18	2.10	1.87	2.02	1.83	1.90	1.92	2.91

[a] Angles are expressed in degrees, distances in Å and energies in kcal/mol.
[b] Definition in ref. 22.
[c] Angles of pseudorotation calculated following ref. 16.
[d] Definition of angles according to fig. 2.

conformations occur on nucleotides situated at the 3′ side of a kink [21]. This similarity with our models may be purely fortuitous, since the kink geometries are quite different; nevertheless, this crystal structure shows that an oligonucleotide duplex can readily adopt the $\alpha^{t}\gamma^{t}$ conformation in order to attenuate strain resulting from the imposition of a deformation.

3.1.7. Hydrogen bonding between NH_3 and the O6 atom of G(5)*

The O6 atoms of the coordinated guanines are possible acceptor atoms for hydrogen bonding donated by the NH_3 ligands. The formation of such bonds is governed by the interplanar angle between the guanine and the PtN_4 plane. The conventions defining this angle [22] have been discussed in detail by Sherman et al. [6b]. It can be seen in fig. 3 of ref. 6b that the 5′-G* can take part in hydrogen-bonding to the NH_3 ligand in the *cis* position, if its interplanar angle with the PtN_4 plane is considerably larger than 90°, whereas for 3′-G*, the condition is that the 3′-G*/PtN_4 angle must be considerably smaller than 90°. The G*/PtN_4 interplanar angles listed in table 1 show that: (i) no hydrogen bonding between NH_3 and G*(4) is possible, since all G*(4)/PtN_4 angles are smaller than 90°; (ii) the best candidates for hydrogen bonding with G*(5) are models C_2 and E_2 which have the smallest G*(5)/PtN_4 angles. The shortest NH · · · O6 distances (table 1) confirm these predictions. However, the values show that even in the case of models C_2 and E_2, the hydrogen bond is rather weak.

3.1.8. Other features of model E_{1A}

In addition to the distinct kink direction ($\phi \approx 30°$), small extent of unwinding, the special position of the C(3)H2′ proton above the plane of the guanine G*(4), and the preference for the $\alpha^{t}\gamma^{t}$ conformation on G*(5), model E_{1A} displays several particular features. Since this model is of great importance for interpretation of the upfield shift of the C(3)H2′ proton [9], these characteristics will now be briefly summarized (table 1):

(i) The interplanar angle between the two coordinated guanines G*(4) and G*(5) is the largest of all the models.

(ii) The interplanar angle between guanine G*(4) and its counterpart C(17) is more than 10° larger than that in the other models.

(iii) The interplanar angles subtended by the PtN_4 plane with the coordinated guanines are the closest to 90°.

(iv) The displacement of the Pt atom from the G*(4) plane is the smallest and that from G*(5) is the largest.

(v) The hydrogen bonds formed between one NH_3 ligand and the phosphate p(4), and between the other NH_3 ligand and T(15)O4, are the shortest.

(vi) The conformation of the C(2) sugar is C4′-*exo* [13,16].

3.1.9. Sequence-dependent features

In both C- and E-models, the kink produces a short repulsive interstrand contact between the two amino groups of cytosines C(3) and C(17). The C(3)H41–C(17)H41 distances are given in table 1. Their lengths are shorter than the sum of the van der Waals radii (2 × 1.20 Å) [23] in all cases except model E_2. In this model the lack of repulsion compensates for the weak interstrand hydrogen bonding (see section 3.1.4).

Generally, such repulsion between amino groups, of course, can occur only in structures where the G*pG* moiety is preceded at the 5′ side by a base possessing an amino group in the major groove, i.e., a cytosine or an adenine. The consequences of replacing the cytosine C(3) by a thymine are discussed below (duplex **2**).

Another sequence-dependent feature is the hydrogen bond formed between one ammine ligand of platinum (that which does not interact with the phosphates) and the O4 atom of thymine T(15) (table 1), which is present in all models except for C_2 and E_2. It seems that in the latter two, the hydrogen bond formed between the other ammine ligand and the phosphate p(3) 'pulls' the *cis*-$Pt(NH_3)_2$ residue to the 5′ side of the platinated strand, preventing the formation of the hydrogen bond with T(15)O4.

Table 2

Geometric parameters and energies of the models for duplex **2** [a]

	Model							
	C_{0N}	C_{0S}	C_1	C_2	E_{0N}	E_{0S}	E_1	E_2
Final energy	−180.5	−174.9	−182.3	−180.3	−181.8	−177.7	−184.9	−181.1
Kink angle (θ) [d]	−64	−65	−64	−66	−61	−61	−61	−61
Unwinding (ψ) [d]	10	9	10	12	4	3	3	4
Kink direction (ϕ) [d]	6	6	6	3	32	33	33	32
Interplanar angles								
C(2)/T(3)	13.0	5.1	13.8	15.7	16.0	16.0	14.6	17.4
T(3)/G*(4)	14.5	10.9	16.7	15.9	17.2	14.1	21.2	18.7
G*(4)/G*(5)	49.5	50.3	49.7	49.7	52.4	52.9	54.5	53.5
G*(5)/A(6)	13.1	10.9	13.1	11.1	10.0	10.5	9.0	10.0
T(3)/A(18)	26.9	19.9	28.0	34.1	28.6	25.4	27.5	37.2
G*(4)/C(17)	27.2	31.3	26.6	27.0	60.0	61.7	62.2	58.1
G*(5)/C(16)	23.9	22.1	23.7	25.4	13.3	13.3	14.3	10.6
C(16)/C(17)	42.5	39.6	42.7	44.5	4.2	4.2	4.0	6.4
C(17)/A(18)	7.2	8.5	7.0	6.8	31.2	34.6	33.6	26.6
G*(4)/PtN_4 [b]	62.6	69.3	62.3	62.3	84.4	81.7	79.7	78.1
G*(5)/PtN_4 [b]	62.8	67.2	64.1	63.6	78.4	78.1	77.1	73.8
Conformation of G*(5) $\alpha\ \gamma$	g−g+	tt	g−g+	g−g+	g−g+	tt	tt	g−g+
Energy difference for $\alpha^-\gamma^+ \rightarrow \alpha^t\gamma^t$	+0.6	−0.2	+0.9	+1.5	+1.9	−0.6	−0.1	+0.5
Sugar puckers [c]								
C(2)	112	113	114	95	53	52	55	31
T(3)	28	144	22	20	37	146	28	24
G*(4)	20	39	12	12	16	33	5	7
G*(5)	141	124	142	128	143	133	125	130
C(16)	31	29	31	32	151	149	150	150
C(17)	150	150	151	143	37	39	36	35
Distance of Pt from G*(4)	0.61	0.54	0.58	0.54	0.58	0.54	0.39	0.42
Distance of Pt from G*(5)	0.35	0.47	0.37	0.42	0.45	0.49	0.57	0.53
Shortest NH ··· O separations								
NH ··· p(3)	3.99	4.17	3.92	2.12	4.02	3.74	4.02	2.15
NH ··· p(4)	3.20	5.13	1.90	2.15	3.43	4.69	1.83	2.16
NH ··· G*(5)O6	2.19	2.58	2.30	2.32	2.93	2.89	2.91	2.72
NH ··· T(15)O4	3.12	2.16	3.24	3.00	1.84	1.86	1.89	1.94
T(3)O4 ··· C(17)H41	2.18	2.12	2.17	2.10	1.96	1.95	1.93	1.96

[a] Angles are expressed in degrees, distances in Å, and energies in kcal/mol.
[b] Definition in ref. 22.
[c] Angles of pseudorotation calculated following ref. 16.
[d] Definition of the angles according to fig. 2.

3.2. Molecular models for the platinated duplex 2

We have replaced the cytosine C(3) in the models for duplex **1** by a thymine, and relaxed the structures. In this way, we have obtained the nine models C_{0N}, C_{0S}, C_1, C_2, E_{0N}, E_{0S}, E_{1A}, E_{1B}, and E_2, for duplex **2**. Model refinement yielded a distinct energy minimum in every case except for

E_{1B}, which refined to a structure similar to that of model E_{1A}. Thus, there is only a single E_1 variant to be distinguished for duplex **2**. The energies of the models and their structural parameters are listed in table 2.

The first striking feature is that all E-models are kinked in the direction of $\phi \approx 30°$, i.e., they belong to the same structural type as model E_{1A} for duplex **1**. This analogy is further demonstrated by the following properties: (i) a small unwinding angle, (ii) a large interplanar angle between G*(4) and C(17), (iii) interplanar angles between the PtN_4 plane and the two G* guanines similar to those of model E_{1A} for duplex **1**, and (iv) the C4'-*exo* conformation [13,16] of nucleotide C(2). The C-models, on the other hand, belong to the same structural type as the C-models for duplex **1**. There is a general decrease in unwinding angle for both C- and E-models. This is, however, due to a difference between the two reference structures (i.e., the refined unplatinated duplexes), rather than to between the platinated models: the unplatinated duplex **1** is wound to a slightly greater extent than the unplatinated duplex **2**.

Fig. 6 shows the central part of models C_1 and E_1. One can see that in the C-models, the T(3)O4 atom forms a bifurcated hydrogen bond to the amino groups of A(18) (its Watson-Crick counterpart) and C(17). Furthermore, the C(17)H41 proton donates a hydrogen bond to both T(3)O4 and G*(4)O6. The E-models, on the other hand, form a short and fairly linear hydrogen bond from C(17)H41 to T(3)O4 (H ··· O distance, 1.93–1.96 Å; N-H ··· O angle, 156–169°), while the G*(4)-C(17) interaction merely consists in formation of the G*(4)H1-C(17)N3 hydrogen bond.

The T(3)O4-C(17)H41 hydrogen bond stabilizes the C- and E-models in geometries which appear to be quite rigid within both families. The structural parameters (table 2) show much less variation among each other for either family than in the case of duplex **1** (table 1). Especially striking is the invariance of angles θ, ψ, ϕ, and of the interplanar angles G*(4)/PtN_4 and G*(5)/PtN_4.

The slightly different geometry of the kink site with respect to that of duplex **1** is reflected in the lengths of the hydrogen bonds formed by the NH_3 ligands of platinum (tables 1 and 2). In particular, the hydrogen bond to T(15)O4 is present and short in length for all E-models for duplex **2**, whereas the C-models show greater NH ··· T(15)O4 separations throughout.

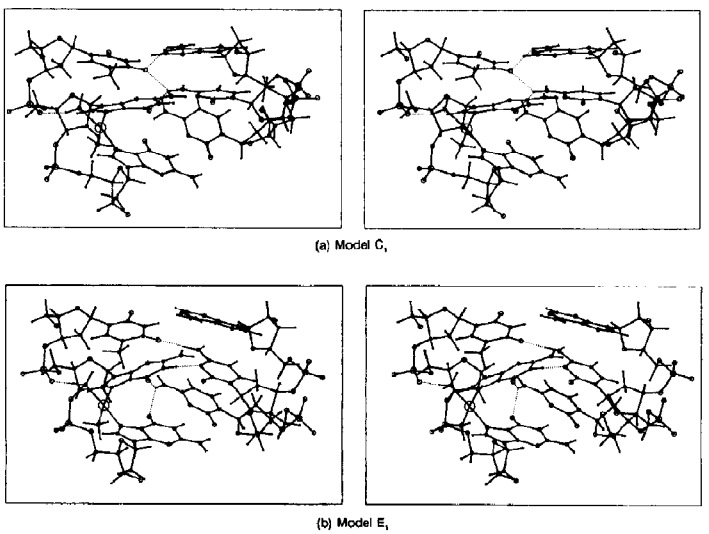

Fig. 6. Stereoview of the central part of duplex **2**, comprising the nucleotides 3–5 and 16–18. Dashed lines indicate hydrogen bonds discussed in the text.

All E-models except E_{0S} suggest the occurrence of significant shielding of the T(3)H2′ proton by the guanine G*(4). The calculated value of the shielding [24] due to all bases, relative to the unplatinated duplex **2**, ranges from 0.7 to 0.9 ppm. With 17 model structures for **1** and **2** now available, we can define the conditions under which the H2′ proton of the nucleotide 5′ to G*G* is placed in the shielding cone of the 5′-G*: (i) the structure must belong to the E-family; (ii) the sugar conformation of the nucleotide 5′ to G*G* must be N; and (iii) the kink direction must be $\phi \approx 30°$. This is an example of how molecular mechanics can help in translating information on chemical shifts into structural characteristics.

On perusal of the data for the sugar puckers of nucleotides 3–5 for duplexes **1** and **2** (tables 1 and 2), one observes that none of the models for duplex **2** shows a negative phase angle (P) for nucleotide 3, as was the case for duplex **1**. A negative phase angle for a deoxyribose manifests itself in distinct values for the $J_{1'2'}$ and $J_{1'2''}$ coupling constants [25] and for duplex **1**, in fact, the C(3) constants $J_{1'2'} = 4.5$ Hz and $J_{1'2''} = 6.5$ Hz are only interpretable if one assumes that a significant contribution is made by a structure with a negative phase angle of C(3). The absence of a conformation having $P < 0°$ on nucleotide 3 should lead to different $J_{1'2'}$ and $J_{1'2''}$ values.

Comparison of the total energies with those for duplex **1** (tables 1 and 2) demonstrates a significant degree of stabilization for model E_1, which has the lowest energy among all models for duplex **2**. This model is thus expected to be the most preponderant conformation of duplex **2**.

4. Conclusion

The molecular modeling of two GpG-platinated oligonucleotide duplexes, compared in one case with a detailed NMR analysis, has shown in the current study that in solution, fluctuations between several conformations take place. However, such conformational changes do not affect the overall shape of the adduct, which is predicted to be kinked by 55–66° towards the major groove and unwound by 3–19°. This is in qualitative agreement with previous observations that cisplatin shortens [26,27] and unwinds [27,28] the DNA double helix, and with recent experiments reported by Rice et al. [29], who investigated the electrophoretic mobilities for multimers of platinated oligonucleotides and their copolymers with a duplex containing an A-tract, and calculated a kink angle of $40 \pm 5°$. The conformations that we have determined by energy minimization differ from one another in the following aspects: (i) the position of the kink in the unplatinated strand which can be opposite the kink in the platinated strand (C-models) or shifted one nucleotide to the 3′ end (E-models); (ii) the number of ammine-phosphate hydrogen bonds (zero to two); and (iii) the direction of the kink axis ($\phi \approx 0$ or $30°$).

A cytosine at the 5′ side of the coordinated G*G* moiety destabilizes the adduct through a short amino-amino contact with the cytosine complementary to the 5′-G*. If the base 5′ to G*G* is a thymine instead of a cytosine, the amino-amino repulsion is replaced by amino-O4 hydrogen bonding, which is predicted to favor energetically the E-model with $\phi \approx 30°$ and one ammine-phosphate hydrogen bond.

A considerable amount of structural work remains to be done in order to gain a better understanding of the antitumor activity of cisplatin. For instance, little is known about other adducts between cisplatin and DNA. We are currently investigating the double-stranded nonanucleotide d(CTCA*G*CCTC)-d(GAGGCTGAG), with a *cis*-$Pt(NH_3)_2$ moiety coordinated to the A* and G* bases, as a model compound for the second adduct of cisplatin with DNA, the ApG cross-link [1]. The cytotoxic and mutagenic effects of this crosslink are different from those in the case of GpG [30]. On elucidation of the structures of cisplatin-DNA adducts, it will be interesting to compare them with those of the DNA adducts formed by compounds that have no antitumor properties. As reported recently, Van Garderen et al. [31] are currently studying the duplex d(TCTCG*TCTC)-d(GAGACGAGA), with $Pt(NH_3)_3^{2+}$ or $Pt(dien)^{2+}$ (dien: diethylenetriamine) bound to the G* guanine, by using ultraviolet, CD and NMR techniques. Monofunctional platinum complexes like $[PtCl(NH_3)_3]Cl$ or

[PtCl(dien)]Cl are inactive against cancer [32]. There is indirect evidence to show that the action of [PtCl(dien)]Cl on DNA does not result in appreciable perturbation of base stacking [26], however, a structural investigation of a monocoordinated duplex is still lacking. A molecular mechanics analysis of the above-mentioned monocoordinated nonamer, carried out as a joint project with Reedijk's group, will hopefully clarify this point.

Supplementary material available

Further data are available from the author on request and comprise tables of sugar pucker and backbone torsional angle parameters (table S1, nine pages) and Cartesian coordinates of all models discussed in the text (on magnetic tape).

Acknowledgements

We thank Dr. M. Le Bret and Dr. J. Gabarro-Arpa for the use of their computer graphics facility, Dr. K. Zimmermann for helpful discussions, Dr. M. Krauss for providing unpublished results on $[Pt(NH_3)_3(gua)]^{2+}$, and Dr. M. Dutreix for the use of the VAX 8600 computer at the Institut Gustave Roussy, Villejuif, France. Stimulating discussions with the members of Professor J. Reedijk's group were made possible thanks to EEC support (grant no. ST2J-0462-C). Financial support from the Ligue Nationale Française Contre le Cancer (J.K.) and the Association pour la Recherche sur le Cancer is gratefully acknowledged.

References

1 a A.M.J. Fichtinger-Schepman, J.L. van der Veer, J.H.J. den Hartog, P.H. Lohman and J. Reedijk, Biochemistry 24 (1985) 707; b A.M.J. Fichtinger-Schepman, A.T. van Oosterom, P.H. Lohman and F. Berends, Cancer Res. 47 (1987) 3000; c A. Eastman, Biochemistry 25 (1986) 3912.
2 A. Laoui, J. Kozelka and J.C. Chottard, Inorg. Chem. 27 (1988) 2751.
3 J.C. Chottard, in: Platinum and other metal coordination compounds in cancer chemotherapy, ed. M. Nicolini (M. Nijhoff, Boston, MA, 1988) p. 53.
4 E. Reed, R.F. Ozols, R. Tarone, S.H. Yuspa and M.C. Poirier, Proc. Natl. Acad. Sci. U.S.A. 84 (1987) 5024.
5 J.M. Pascoe and J.J. Roberts, Biochem. Pharmacol. 23 (1974) 1345.
6 a S.E. Sherman, D. Gibson, A.H.J. Wang and S.J. Lippard, Science 230 (1985) 412; b S.E. Sherman, D. Gibson, A.H.J. Wang and S.J. Lippard, J. Am. Chem. Soc. 110 (1988) 7368.
7 G. Admiraal, J.L. van der Veer, R.A.G. de Graaff, J.H.J. den Hartog and J. Reedijk, J. Am. Chem. Soc. 109 (1987) 592.
8 a J. Kozelka, G.A. Petsko, G.J. Quigley and S.J. Lippard, J. Am. Chem. Soc. 107 (1985) 4079; b J. Kozelka, G.A. Petsko, G.J. Quigley and S.J. Lippard, Inorg. Chem. 25 (1986) 1075; c J. Kozelka, S. Archer, G.A. Petsko, G.J. Quigley and S.J. Lippard, J. Biopolymers 26 (1987) 1245.
9 F. Herman, J. Kozelka, V. Stoven, E. Guittet, J.P. Girault, T. Huynh-Dinh, J. Igolen, J.Y. Lallemand and J.C. Chottard, submitted for publication.
10 IUPAC-IUB Joint Commissions on Biochemical Nomenclature Report, Eur. J. Biochem. 131 (1983) 9.
11 a P. Weiner and P. Kollman, J. Comput. Chem. 2 (1981) 287; b S.J. Weiner, P.A. Kollman, D.T. N'guyen and D.A. Case, J. Comput. Chem. 7 (1986) 230.
12 Definitions and Nomenclature of Nucleic Acid Structure Parameters, J. Mol. Biol. 205 (1989) 787.
13 W. Saenger, Principles of nucleic acid structure (Springer, New York, 1984) ch. 2.
14 a J. Reedijk, A.M.J. Fichtinger-Schepman, A.T. van Oosterom and P. van de Putte, Struct. Bond. 67 (1987) 53; b S.E. Sherman and S.J. Lippard, Chem. Rev. 87 (1987) 1153.
15 M. Krauss, H. Basch and K.J. Miller, J. Am. Chem. Soc. 110 (1988) 4517.
16 C. Altona and M. Sundaralingam, J. Am. Chem. Soc. 95 (1972) 8205.
17 H.M. Sobell, C. Tsai, S.G. Gilbert, S.C. Jain and T.D. Sakore, Proc. Natl. Acad. Sci. U.S.A. 73 (1976) 3068.
18 H.M. Sobell, C. Tsai, S.C. Jain and S.G. Gilbert, J. Mol. Biol. 114 (1977) 333.
19 D.G. Gorenstein, Phosphorus-31 NMR (Academic Press, Orlando, FL, 1984) ch. 8.
20 C. Spellmeyer-Fouts, L.G. Marzilli, R.A. Byrd, M.F. Summers, G. Zon and K. Shinozuka, Inorg. Chem. 27 (1988) 366.
21 A.C. Dock-Bregeon, B. Chevrier, A. Podjarny, D. Moras, J.S. deBear, G.R. Gough, P.T. Gilham and J.E. Johnson, Nature 335 (1988) 375.
22 J.D. Orbell, L.G. Marzilli and T.J. Kistenmacher, J. Am. Chem. Soc. 103 (1981) 5126.
23 A. Bondi, J. Phys. Chem. 68 (1964) 441.
24 a C. Giessner-Prettre, B. Pullman, P.N. Borer, L.-S. Kan and P.O.P. Ts'o, Biopolymers 15 (1976) 2277; b C. Giessner-Prettre and B. Pullman, Q. Rev. Biophys. 20 (1987) 113.
25 L.J. Rinkel and C. Altona, J. Biomol. Struct. Dyn. 4 (1987) 621.
26 J.P. Macquet and J.-L Butour, Biochimie 60 (1978) 901.
27 a G.L. Cohen, W.R. Bauer, J.K. Barton and S.J. Lippard,

Science 203 (1979) 1014; b C.M. Merkel and S.J. Lippard, Cold Spring Harbor Symp. Quant. Biol. 47 (1983) 355.
28 a W.M. Scovell and L.R. Kroos, Biochem. Biophys. Res. Commun. 104 (1982) 1597; b W.M. Scovell and F. Collart, Nucleic Acids Res. 13 (1985) 2881.
29 J.A. Rice, D.M. Crothers, A.L. Pinto and S.J. Lippard, Proc. Natl. Acad. Sci. U.S.A. 85 (1988) 4158.
30 a D. Burnouf, M. Daune and R.P.P. Fuchs, Proc. Natl. Acad. Sci. U.S.A. 84 (1987) 3758; b D. Burnouf, C. Gauthier, J.-C. Chottard and R.P.P. Fuchs, Proc. Natl. Acad. Sci. U.S.A., in the press.
31 C.J. van Garderen, L.P.A. van Houte, H. van den Elst, J.H. van Boom and J. Reedijk, J. Am. Chem. Soc. 111 (1989) 4123.
32 a J.-P. Macquet and J.-L Butour, J. Natl. Cancer Inst. 70 (1983) 899; b M.J. Cleare and J.D. Hoeschele, Bioinorg. Chem. 2 (1973) 187.